NIH Public Access
Author Manuscript
Biochem J. Author manuscript; available in PMC 2014 December 15.

Published in final edited form as:
Biochem J. 2013 December 15; 456(3): 453–462. doi:10.1042/BJ20131163.

NRMT2 is an N-terminal monomethylase that primes for its homolog NRMT1

Janusz J. Petkowski[*], **Lindsay A. Bonsignore**[†], **John G. Tooley**[†], **Daniel W. Wilkey**[‡], **Michael L. Merchant**[‡], **Ian G. Macara**[§], and **Christine E. Schaner Tooley**[†,1]

[*]Department of Biology (D-BIOL), Institute of Biochemistry (IBC), ETH Zurich, Zurich 8093, Switzerland [†]Department of Biochemistry & Molecular Biology, University of Louisville School of Medicine, Louisville, KY 40202, U.S.A [‡]Clinical Proteomics Center, University of Louisville, Louisville, KY 40202, U.S.A [§]Department of Cell & Developmental Biology, Vanderbilt University, Nashville, TN 37232, U.S.A

Abstract

N-terminal RCC1 methyltransferase (NRMT) was the first eukaryotic methyltransferase identified to specifically methylate the free α-amino group of proteins. Since the discovery of this N-terminal methyltransferase, many new substrates have been identified and the modification itself has been shown to regulate DNA-protein interactions. Sequence analysis predicts one close human homolog of NRMT, Methyltransferase-like protein 11B (METTL11B, now renamed NRMT2). We show here for the first time that NRMT2 also has N-terminal methylation activity and recognizes the same N-terminal consensus sequences as NRMT (now NRMT1). Both enzymes have similar tissue expression and cellular localization patterns. However, enzyme assays and mass spectrometry experiments indicate they differ in their specific catalytic functions. While NRMT1 is a distributive methyltransferase that can mono-, di-, and trimethylate its substrates, NRMT2 is primarily a monomethylase. Concurrent expression of NRMT1 and NRMT2 accelerates the production of trimethylation, and we propose that NRMT2 activates NRMT1 by priming its substrates for trimethylation.

Keywords

methylation; methyltransferase; Regulator of Chromatin Condensation 1 (RCC1); N-terminal RCC1 methyltransferase 1 (NRMT1); N-terminal RCC1 methyltransferase 2 (NRMT2)

[1]Corresponding Author: Christine E. Schaner Tooley, Department of Biochemistry & Molecular Biology, University of Louisville School of Medicine, Louisville, KY 40202, U.S.A. Telephone: (502) 852-0322, Fax: (502) 852-6222. cescha05@louisville.edu.

AUTHOR CONTRIBUTIONS

Janusz Petkowski did the homology modeling experiments, the NRMTI and NRMTII rescue experiments, the GFP localization experiments, and the testing of the NRMTII consensus sequence. He also contributed greatly to the intellectual design of the project. Lindsay Bonsignore did the qRT-PCR experiments. John Tooley prepared the mass spectrometry samples and did the enzyme assays. Daniel Wilkey and Michael Merchant performed and analyzed the mass spectrometry experiments. Ian Macara and Christine Schaner Tooley directed the experiments, and Christine Schaner Tooley wrote the manuscript.

NIH-PA Author Manuscript
NIH-PA Author Manuscript
NIH-PA Author Manuscript

NIH-PA Author Manuscript

NIH-PA Author Manuscript

NIH-PA Author Manuscript

INTRODUCTION

N-terminal methylation of free α amino groups had been documented for many decades, but very little was known about the function of this modification [1]. Of the few eukaryotic proteins known to be N-terminally methylated, almost all contained an N-terminal X-Pro-Lys consensus sequence (Rubisco being an exception [2]), indicating that one specific enzyme might be responsible for this post-translational modification [1]. The first functional role of N-terminal methylation was determined by mutating the Ser-Pro-Lys consensus of the Ran guanine nucleotide exchange factor Regulator of Chromatin Condensation 1 (RCC1) [3]. This resulted in loss of RCC1 N-terminal methylation, decreased affinity of RCC1 for DNA, mislocalization of RCC1 during mitosis, and the formation of multi-polar spindles [3]. It has also recently been shown that the N-terminal glycines of CENP-A and CENP-B are N-terminally methylated [4, 5]. N-terminal methylation of CENP-B regulates its binding to centromeric DNA [5], and N-terminal methylation of CENP-A likely helps regulate the phasing of CENP-A nucleosomes on centromeric α-satellite DNA [4]. In addition to regulation of protein-DNA binding, many N-terminally methylated proteins are found in large multi-subunit complexes with their N-termini at locations of contact to neighboring proteins, signifying this modification may also play a role in the regulation of protein-protein interactions [1]. N-terminal methylation is also protective against digestion by cellular aminopeptidases [6] and may interfere with N-terminal acetylation and the N-end rule pathway [7, 8], indicating a role in protein stability.

The first eukaryotic N-terminal methyltransferase, NRMT/NTMT (now NRMT1), was identified as the enzyme that methylates the N-termini of RCC1 [9] and the ribosomal proteins Rpl12 and Rps25 [10]. Accordingly, NRMT1 loss in human embryonic kidney cells results in decreased RCC1 localization to chromatin and increased multi-polar spindle formation during mitosis [9]. Yeast lacking NRMT1 have altered ribosomal profiles and defects in translational fidelity and efficiency [11]. We have previously shown that NRMT1 mono-, di-, and trimethylates an N-terminal X-Pro-Lys (X-P-K) consensus sequence, with X being any amino acid other than Leu, Ile, Trp, Asp, or Glu [9]. Using this consensus sequence, we have also confirmed a variety of new NRMT1 substrates, including the tumor suppressor Retinoblastoma protein (RB), the oncoprotein SET, the transcription factor Kelch-like protein 31, and numerous myosin light chains and ribosomal proteins [9]. Though NRMT1 substrates are numerous and predominantly abundant proteins, NRMT1 itself is ubiquitously expressed at considerably low levels (Figure 5C), suggesting there may be an additional enzyme(s) capable of N-terminal methylation.

NRMT1 (formerly METTL11A) is a member of the Class I Methyltransferase family, as it lacks a SET domain (common of the histone methyltransferases) and is composed of a seven beta-strand structure. Sequence analysis indicates one close human homolog, Methyltransferase-like protein 11B (now renamed NRMT2) [10]. Characterization of other methyltransferase families has shown that such close homologs usually differ in either their expression/localization patterns or their catalytic activity. For example, PRMT1 and PRMT8 are both type I arginine methyltransferases from the protein arginine methyltransferase (PRMT) family. They both methylate glycine/arginine-rich motifs, however, PRMTI is ubiquitously expressed and PRMT8 is specifically expressed in the brain [12]. PRMT8 is

NIH-PA Author Manuscript

NIH-PA Author Manuscript

NIH-PA Author Manuscript

also myristoylated, resulting in membrane-specific localization [12]. In comparison, the nuclear receptor-binding SET domain proteins NSD1 and NSD2 are both nuclear histone methyltransferases. However, NSD1 is a histone H3 lysine 36 dimethylase [13], while NSD2 is a histone H3 lysine 36 trimethylase [14].

Here we report that NRMT2 is a functional N-terminal methyltransferase that also recognizes and methylates an X-P-K consensus sequence. NRMT1 and NRMT2, analogous to the NSD family of methyltransferases, have similar localization and expression patterns but differ in their catalytic activity. NRMT1 is a distributive methyltransferase that can mono-, di-, and trimethylate its substrates, while NRMT2 is primarily a monomethylase. We propose a model whereby their similar localization patterns allow NRMT2 to prime for NRMT1, allowing for quicker and more robust di- and trimethylation of substrates. This regulatory mechanism would be especially useful in tissues with a high abundance of substrates.

MATERIALS AND METHODS

Constructs and antibodies

The SPK and APK-RCC1 substrates for determining NRMT2 consensus specificity were expressed from a modified pet15b vector (Novagen) and were processed by Factor X cleavage and purified as previously described [9]. The PPK-RCC1 substrate was expressed in pet30a as previously described[3]. Human *NRMT1* and mouse *NRMT2* (Open Biosystems) were cloned into the XbaI and BamHI sites of pKGFP2 to remove one copy of GFP and create the NRMT1-GFP and NRMT2-GFP constructs for cellular localization experiments. Human NRMT1 and human NRMT2 (Open Biosystems) were cloned into the NdeI and XhoI sites of pet15b for production of recombinant protein. The recombinant human RCC1 substrate was expressed in pET30a [3]. All His-tagged proteins were purified as previously described [15].

Primary antibodies used for western blot analysis are as follows: 1:20,000 rabbit anti-trimethylated SPK-RCC1 (me3-RCC1)[3], 1:10,000 rabbit anti-mono/dimethylated SPK-RCC1 (me1/2-RCC1) [3], 1:1000 rabbit anti-dimethylated PPK-RCC1 (me2-PPK), 1:1000 goat anti-RCC1 (Santa Cruz Biotechnology, Inc., sc-1162), 1:1000 rabbit anti-NRMT1 [9], and 1:3000 mouse anti-beta-catenin (BD Biosciences).

NRMT2 rescue assay

Lentivirus was produced through calcium-phosphate transfection of 2.5×10^6 human embryonic kidney (HEK) 293LT cells with the viral envelope plasmid pMD2.G, the viral packaging vector psPAX2, and pGIPZ (Open Biosystems) containing the shRNAmir and/or the rescuing cDNA. 10,000 293LT cells were infected with lentivirus (control, NRMT1 shRNAmir, NRMT1 shRNAmir co-expressing murine NRMT1–Flag or NRMT1 shRNAmir co-expressing murine NRMT2–Flag) to an MOI of 3. The cells were grown for 2 days and transduced cells were selected by addition of 2 μg ml^{-1} puromycin. The cells were grown two additional days and lysed in lysis buffer (500 mM NaCl; 50 mM Tris pH 8.0; 5 mM

NIH-PA Author Manuscript

NIH-PA Author Manuscript

NIH-PA Author Manuscript

$MgCl_2$; 1 mM EDTA; 1 mM EGTA; 0.1% NP-40; BME and protease inhibitors). Each lysate (50 μg) was analyzed by western blot.

In vitro methylation assays

In vitro methylation reactions with Factor X digested substrates were done as described previously [9]. For the assays determining catalytic specificity (both by western blot and mass spectrometry), 1 μg recombinant human enzyme was mixed with 1 μg recombinant RCC1 substrate in the presence of 100 μM S-adenosylmethionine (AdoMet) (Sigma-Aldrich). The reaction volume was brought to 20 μl with methyltransferase (MTase) buffer (50 mM Tris, pH 8; 50 mM potassium acetate). Each reaction was run for 60 min at 30°C to ensure reaction ran to completion. For mechanistic studies, 25–500 ng of recombinant enzyme was mixed with 1–2 μg recombinant RCC1 substrate in the presence of 100 μM AdoMet. Reaction volume was adjusted to 20 μl with MTase buffer and run from 2.5 to 30 minutes at 30°C depending on the experiment. 5 μl of the total reaction was analyzed in each lane of the western blots. Measurements of mono/di- and trimethylation of RCC1 were done on the same reactions. Western blot images were taken with the ChemiDoc MP Imaging System (Bio-Rad) and % RCC1 trimethylation was quantified using Image Lab (Bio-Rad) software. Briefly, identical boxes were used to measure the intensity of each trimethylated band and corresponding total RCC1 loading control. The methylated intensity was divided by the total RCC1 intensity and multiplied by 100 to give % RCC1 trimethylation.

Mass Spectrometry Analysis

The analysis for the presence and extent of RCC1 N-terminal methylation was conducted as described by Chen et al. with some modifications [3]. *In vitro* methylated RCC1 proteins were resolved on SDS PAGE gels and bands visualized using Coomassie Blue stain. The gel bands were excised, de-stained and equilibrated into 0.1M triethylammonium bicarbonate, pH 8.5 and digested with 100ng Asp-N (Roche, Palo Alto, CA) per gel plug. The digest supernatant was transferred to a new tube and the gel plugs extracted using a modification of Shevchenko et al [16]. The digest and extract were combined, dried by SpeedVac (Savant, Thermo Scientific, Waltham, MA) and re-suspended in 20μL of 0.1% formic acid/2% acetonitrile and then filtered through 0.2um regenerated cellulosic syringe filters (National Scientific, Thermo Scientific, Waltham, MA). A 5ul aliquot of this peptide solution was loaded onto a Dionex Acclaim PepMap 100 75μm × 2cm, nanoViper (C18, 3μm, 100Å) trap, and resolved on a Dionex Acclaim PepMap RSLC 50μm × 15cm, nanoViper (C18, 2μm, 100Å) separating column. The sample was eluted using a linear 2% to 60% acetonitrile gradient using an EASY nano1000 UHPLC and introduced into a LTQ-Orbitrap ELITE mass spectrometer (ThermoElectron, Waltham, MA) for accurate mass measurements using a Nanospray Flex Ion Source (ThermoElectron, Waltham, MA), a stainless steel emitter with a capillary temperature set to 225 C and a spray voltage of 1.6kV and lock mass enabled (0% lock mass abundance) for the 371.101236m/z polysiloxane peak as an internal calibrant [17]. Tandem mass spectra were collected using HCD and ETD fragmentation using an Nth Order Double Play with ETD Decision Tree method [18] was created in Xcalibur v2.2. Targeted and data dependent spectra were acquired and searched using MASCOT ver 2.1 through Proteome Discoverer 1.4 considering up to two missed cleavages, as well as phosphorylation and N-terminal methylation as variable modifications. All spectra MS2 for

NIH-PA Author Manuscript

NIH-PA Author Manuscript

NIH-PA Author Manuscript

RCC1 were manually interpreted. Extracted ion chromatograms for the +2, +3 and +4 charge states for individual N-terminal RCC1 peptides were aggregated and used to estimate relative abundances of modified and unmodified, normal and des-Met truncated N-terminal RCC1 peptides.

NRMT1 and NRMT2 Localization

For live cell imaging, HeLa cells were plated in 2-well Lab-Tek II coverglass (Nunc) in DMEM/F12 50/50 without phenol red (Cellgro) supplemented with 10% FBS (Gibco) and transiently transfected with 2.0 μg NRMT1-GFP, NRMT2-GFP, or pKGFP-GFP using Lipofectamine 2000 (Invitrogen). After 24 hrs, cells were counterstained with DRAQ5 dye (1 μg ml^{-1}), Imaging was performed on a Zeiss LSM510 Meta confocal microscope, using a 100x oil immersion lens (na 1.3), at 512×512 pixel resolution, and a zoom of 2.0. Images were processed and quantified using ImageJ 1.41b software.

Quantification of mRNA in mouse tissue

RNA isolation was performed by homogenization of tissues in TRIzol (Life Technologies) using the Powermax™ Advanced Homogenizing System 200 (VWR). Samples were then mixed with chloroform to extract RNA, the RNA was pelleted using isopropanol, and then washed with ethanol. cDNA was synthesized using the SuperScript First-Strand Synthesis System (Invitrogen). Quantitative RT-PCR was performed with SYBR green PCR Master Mix and the CFX96 Touch™ Real-Time PCR Detection System and Sequence Detection Software (Bio-Rad). Primers (Integrated DNA Technologies) were designed using Primer 3 v 0.4.0. Primers sequences were 5′-TCT TCC CCC AGG TAG CTC T-3, 5′-TGC AGA GGT TTT TAA GGG AAG-3′ for NRMT1 and 5′-CTT TCA GAG CTA CCT CTA CC-3′, 5′-GAA ATT CAC GAG AGG CTT GG-3′ for NRMT2. Gene expression was analyzed using a standard curve as previously described [19], as there were no housekeeping controls expressed at comparably low levels and constant between tissues. All real-time PCR assays included analysis of melting curves and agarose gel electrophoresis to confirm the presence of single PCR reaction products. The identity of NRMT1 and NRMT2 real-time PCR products was confirmed by sequencing (DNA Sequencing Core, University of Louisville, Louisville, KY).

RESULTS

Substrate specificity of NRMT2 is similar to NRMT1

NRMT1 has one close human homolog METTL11B [10], which we renamed NRMT2. The amino acid sequence identity between NRMT1 and NRMT2 is close to 50%, with all the catalytic residues being fully conserved (Figure 1). NRMT2 has an additional 60 amino acid N-terminal domain, which likely has a structure comprised of two helices (Figure 2A). Homology modeling by the Robetta server [20] showed that the overall fold of the catalytic domain of NRMT2 is highly similar to NRMT1 (RMSD less than 2.0Å), with all the critical catalytic residues occupying the same spatial positions (Figure 2B). We have previously shown that Asn169, Asp178, Asp181, and Ser183 are needed for the catalytic activity of NRMT1 [9], and the homology modeling places the corresponding Asn223, Asp232, Asp235, and Ser237 of NRMT2 in almost identical positions in the catalytic site (Figure

NIH-PA Author Manuscript

NIH-PA Author Manuscript

NIH-PA Author Manuscript

2B). The modeling also reveals conserved aromatic residues in the active sites of NRMT1 and NRMT2 (Figure 2C) that are reminiscent of the aromatic residues of chromodomains and may be responsible for binding methylated substrates or products [7].

Sequence and structural similarity of NRMT1 to NRMT2 suggest that these two enzymes likely have similar enzymatic activities and substrate specificities. To test if NRMT2 is capable of methylating SPK, PPK or APK N-terminal consensus sequences (which can all be recognized by our me2-PPK RCC1 antibody), we employed a system in which Factor X cleavage provides efficient exposure of the residue to be methylated [9]. *In vitro* methylation assays showed that recombinant NRMT2 is capable of methylating SPK, PPK and APK recombinant substrates (Figure 3A). Furthermore, C-terminally FLAG-tagged murine NRMT2 expressed in 293LT cells is capable of rescuing NRMT1 knockdown and restoring efficient RCC1 αN-methylation, indicating the enzymes have overlapping catalytic activities (Figure 3B). However, we had previously seen that rescuing NRMT1 knockdown with NRMT1-FLAG restores both RCC1 mono/di- and trimethylation [9], but rescue with NRMT2-FLAG only restores RCC1 mono/dimethylation (Figures 3B and C).

Catalytic Activity of NRMT2 differs from NRMT1

To verify the rescue experiments indicating NRMT2 does not have trimethylase activity, we performed *in vitro* methylation assays with recombinant human NRMT1 or recombinant human NRMT2 as the enzyme and recombinant human RCC1 as the substrate. The reaction was done for 60 minutes at 30°C in the presence of 100 μM AdoMet with 1 μg each of enzyme and substrate. These conditions were chosen to ensure the reaction went to completion and the amount of enzyme was not rate limiting. The reaction was then run on an SDS-polyacrylamide gel and analyzed by western blot with anti-me1/2RCC1 and anti-me3RCC1 antibodies. After 60 minutes, little RCC1 mono/dimethylation is seen following incubation with NRMT1, but higher levels are seen with NRMT2 (Figure 4A). In contrast, when looking at RCC1 trimethylation, there are high levels following incubation with NRMT1, but none after NRMT2 treatment (Figure 4A). These data indicate that after 60 minutes, NRMT1 is capable of almost completely trimethylating RCC1, while NRMT2 can only complete dimethylation.

As the me1/2-RCC1 antibody recognizes both mono- and dimethylation, we wanted to use mass spectrometry (MS) to verify that NRMT2 was capable of both N-terminal mono- and dimethylation. The same *in vitro* methylation reactions were performed as above, run on an SDS-polyacrylamide gel, and stained with Coomassie brilliant blue. The RCC1 protein band was excised and analyzed for N-terminal methylation by MS. As is observed by western blot, LC-MS/MS analysis indicated that the NRMT1 reaction produced almost complete trimethylation of RCC1 (Figure 4B and Supplemental Figure 1). However, surprisingly the NRMT2 reaction only produced significant levels of monomethylation (Figure 4C and Supplemental Figure 1), indicating NRMT2 is primarily an N-terminal monomethylase.

NRMT2 Localization and Tissue Expression

Now knowing that NRMT1 and NRMT2 have different catalytic activities, we were interested in determining if they also have different cellular localization patterns. We tagged

NIH-PA Author Manuscript

NIH-PA Author Manuscript

NIH-PA Author Manuscript

NRMT2 with green fluorescent protein (GFP) and expressed it in HeLa cells. Similarly to NRMT1 [9] (Figure 5A), immunofluorescent analysis shows NRMT2 is enriched in the nuclear compartment as compared to a GFP-GFP control protein (Figure 5A). The nuclear to cytoplasmic ratio of NRMT1 and NRMT2 was also quantified and found to be significantly different than that of the GFP-GFP control (Figure 5B).

As we determined that NRMT1 and NRMT2 have similar cellular localization patterns, we next analyzed their tissue distribution. Quantitative Real-time PCR (qRT-PCR) analysis was performed for both NRMT1 and NRMT2 in mouse tissue lysates. Both enzymes are expressed at fairly low levels in all tissues examined (approximately 100–200 copies of transcript per 40 ug of cDNA). However, NRMT1 mRNA is enriched in the brain, NRMT2 mRNA is enriched in the liver, and both are enriched in skeletal muscle (Figures 5C and D). Due to the low expression levels, we confirmed the specificity of the NRMT1 and NRMT2 qRT-PCR reactions by sequencing the products to verify that the correct targets were amplified (data not shown).

NRMT2 primes for NRMT1

To establish a functional distinction between two N-terminal methyltransferase family members that have such similar subcellular localization and tissue expression profiles, we performed enzyme assays with NRMT1 and NRMT2 individually or in combination. We hypothesized that one reason for overlapping localization and expression patterns is that NRMT1 and NRMT2 are working synergistically. Lysine methylation has been shown to occur by one of two mechanisms, processive or distributive [21]. Processive methyltransferases can add up to three methyl groups without dissociation from the substrate. Therefore trimethylation by these enzymes is not dependent on the concentration of previously mono- or dimethylated substrate. In contrast, distributive methyltransferases add a methyl group, then must dissociate from the substrate before additional methyl groups can be added [21]. Increasing the amount of previously mono- or dimethylated substrate can thereby increase di- or trimethylation by these methyltransferases.

The complex pattern of RCC1 N-terminal methylation in mammalian cells (5% unmethylated, 20% monomethylated, 30% dimethylated, and 45% trimethylated) [3] indicates that NRMT1 is distributive or has an extremely low k_{cat}. If NRMT1 is distributive, NRMT2 should be able to increase NRMT1 di- and trimethylation activity by increasing the pool of monomethylated substrates available. This would be especially useful in the presence of high concentrations of substrate.

We analyzed the methylation mechanisms of NRMT1 and NRMT2 by performing *in vitro* methylation assays with increasing concentrations of recombinant enzyme and a constant concentration of substrate (recombinant human RCC1). If the reaction time is kept constant, a processive enzyme will produce different amounts of only one methylation state. However, a distributive enzyme will produce all three methylation sites, with the highest order of methylation occurring slowly and dependent on the concentration of enzyme [21]. As shown in Figure 6A, at low concentrations of NRMT1 we first observe robust RCC1 mono/dimethylation. Increasing the concentration of NRMT1 results in a gradual accumulation of RCC1 trimethylation with a corresponding decrease in RCC1 mono/

NIH-PA Author Manuscript

NIH-PA Author Manuscript

NIH-PA Author Manuscript

dimethylation (Figure 6A). The appearance of both mono/di- and trimethylation, the order in which they appear, and the eventual decrease of RCC1 mono/dimethylation indicate that NRMT1 is a distributive trimethylase.

In contrast, when using NRMT2 as the enzyme, we only observe RCC1 mono/dimethylation, which we now know from the mass spectrometry data is predominantly monomethylation (Figure 6B). These levels rise with increasing concentration of NRMT2 and do not decrease at high levels of enzyme, as seen with NRMT1. We do not see the appearance of RCC1 trimethylation (Figure 6B), further confirming NRMT2 is not a trimethylase. When NRMT1 and NRMT2 are combined in a reaction, RCC1 trimethylation appears more rapidly and intensely (Figures 6C and D), indicating that NRMT2 can serve as an activator/primer for NRMT1 trimethylation.

DISCUSSION

These experiments verify for the first time that NRMT2 is an N-terminal methyltransferase, that it has a different catalytic specificity from its homolog NRMT1, and that it can prime NRMT1 substrates for higher degrees of methylation. NRMT1 and NRMT2 are not the first highly similar methyltransferase family members to differ in their specific catalytic functions. The nuclear receptor SET domain-containing methyltransferases NSD1, NSD2, and NSD3 are almost identical in a 700 amino acid stretch (including their catalytic domain), yet bind histone H3 differently and catalyze different levels of methylation at lysine 36 [13, 14, 22]. Structural studies indicate the differences in the NSD methyltransferases comes from their chromatin binding motifs, which target them to different promoter regions [22]. Comparison of NRMT1 crystal structure and NRMT2 homology model indicate that the main region of variance between the two homologs is the additional N-terminal domain of NRMT2. These additional bulky helices could easily prevent binding of NRMT2 to previously methylated substrates. Thus, it will be interesting to see if deleting the N-terminal domain of NRMT2 will allow it to di- and trimethylate its substrates. It would also be interesting to determine if switching the conserved trio of aromatic residues in the active sites of NRMT1 and NRMT2 could switch their catalytic activities. Though similar in structure (Figure 2C), the exact residues differ slightly and could dictate binding of unmethylated versus mono- or dimethylated substrates (see EZH2 below) [23].

The inability of NRMT2 to di- or trimethylate X-P-K substrates *in vitro* indicates that it is primarily a monomethylase. However, NRMT1 is capable of trimethylation *in vitro*, demonstrating the two enzymes do have inherent catalytic differences and may be differentially regulated. For example, the monomethylase activity of NRMT2 may protect it from product feedback inhibition. We have previously shown NRMT1 can bind to and become inhibited by its di- and trimethylated products [7]. As NRMT2 is not able to di- and trimethylate substrates, it is also unlikely to bind these products. Di- and trimethylated species constitute the majority of N-terminally methylated proteins in the cell [3], so NRMT2 expression could be used to alleviate or bypass this inhibition. This would be especially useful in tissues like skeletal muscle, which contains high amounts of trimethylated myosin proteins [9]. Higher NRMT2 expression in skeletal muscle (Figure

NIH-PA Author Manuscript

NIH-PA Author Manuscript

NIH-PA Author Manuscript

5D) may aid NRMT1 strained by substrate burden and product inhibition. It is currently unclear why NRMT1 mRNA is enriched in the brain and NRMT2 mRNA is enriched in the liver. However, these unique aspects of their expression patterns suggest they are serving non-redundant, tissue-specific functions.

In addition, loss of NRMT1 activity alone has phenotypic consequences both *in vitro* [9] and *in vivo* (C.S.T unpublished data), indicating NRMT1 and NRMT2 have non-redundant roles during cell growth and development. These data also demonstrate that N-terminal monomethylation and di/trimethylation serve non-redundant functions. There is mounting evidence of distinct functional roles for different levels of histone methylation, with the extent of methylation often controlling the binding of effector proteins [24]. There is also evidence that disruption of these levels has extreme biological effects. The histone methyltransferase EZH2 is predominantly a histone H3 lysine 27 (H3K27) monomethylase [23]. However, in a subset of follicular lymphoma and diffuse-large B-cell lymphomas there is a gain-of-function tyrosine to phenylalanine mutation at amino acid 641 (Y641F) in the active site that turns EZH2 into a H3K27 trimethylase [23]. It is proposed that this change in methylation ability alters the transcriptions levels of different tumor suppressors regulated by EZH2, leading to the progression of B-cell tumorigenesis [23].

In the same way, mutations that alter the expression levels or catalytic functions of NRMT1 or NRMT2 could produce developmental defects and lead to disease. In fact, mutations in both NRMT1 and NRMT2 have been found in a variety of cancers, including point mutations in the NRMT2 active site [25–27] (Cosmic Catalogue of Somatic Mutations in Cancer). NRMT1 is overexpressed in colon and rectal cancers [28, 29], indicating an increase in di/trimethylated substrates may exacerbate the pathology of these diseases. However, in breast cancer, NRMT1 expression is more often decreased [30–32], indicating di/trimethylated substrates may be protective against this pathology or an increase in monomethylated substrates may be particularly detrimental. It will be interesting to now analyze NRMT2 levels in these disease states and see how they correspond, and to determine if NRMT1 and NRMT2 mutations are commonly found in the same tumor samples. It will also be interesting to identify exactly which N-terminally methylated targets play a role in each disease state and to determine if the particular targets differ between cancer types.

Supplementary Material

Refer to Web version on PubMed Central for supplementary material.

Acknowledgments

The authors would like to thank the University of Louisville Quantitative Mass Spectrometry Core Proteomics Facility for their careful and expedient processing of samples. The authors declare no competing financial interests.

FUNDING

This work was supported by research grants from the National Institutes of Health to C.E.S.T. [CA158009] and I.G.M [GM50526].

NIH-PA Author Manuscript

NIH-PA Author Manuscript

NIH-PA Author Manuscript

Abbreviations

CENP-A	Centromere protein A
CENP-B	Centromere protein B
MOI	multiplicity of infection
AdoMet	S-adenosylmethionine
SAH	S-adenosylhomocysteine
NSD	nuclear receptor SET domain-containing
EZH2	enhancer of zeste homolog 2

References

1. Stock A, Clarke S, Clarke C, Stock J. N-terminal methylation of proteins: structure, function and specificity. FEBS Lett. 1987; 220:8–14. [PubMed: 3301412]
2. Grimm R, Grimm M, Eckerskorn C, Pohlmeyer K, Rohl T, Soll J. Postimport methylation of the small subunit of ribulose-1,5-bisphosphate carboxylase in chloroplasts. FEBS Lett. 1997; 408:350–354. [PubMed: 9188792]
3. Chen T, Muratore TL, Schaner-Tooley CE, Shabanowitz J, Hunt DF, Macara IG. N-terminal alpha-methylation of RCC1 is necessary for stable chromatin association and normal mitosis. Nat Cell Biol. 2007; 9:596–603. [PubMed: 17435751]
4. Bailey AO, Panchenko T, Sathyan KM, Petkowski JJ, Pai PJ, Bai DL, Russell DH, Macara IG, Shabanowitz J, Hunt DF, Black BE, Foltz DR. Posttranslational modification of CENP-A influences the conformation of centromeric chromatin. PNAS. 2013; 110:11827–11832. [PubMed: 23818633]
5. Dai X, Otake K, You C, Cai Q, Wang Z, Masumoto H, Wang Y. Identification of Novel alpha-N-Methylation of CENP-B That Regulates Its Binding to the Centromeric DNA. J Proteome Res. 2013; 12:4167–4175. [PubMed: 23978223]
6. Pettigrew GW, Smith GM. Novel N-terminal protein blocking group identified as dimethylproline. Nature. 1977; 265:661–662. [PubMed: 193025]
7. Petkowski JJ, Schaner Tooley CE, Anderson LC, Shumilin IA, Balsbaugh JL, Shabanowitz J, Hunt DF, Minor W, Macara IG. Substrate specificity of mammalian N-terminal alpha-amino methyltransferase NRMT. Biochemistry. 2012; 51:5942–5950. [PubMed: 22769851]
8. Varshavsky A. The N-end rule: functions, mysteries, uses. PNAS. 1996; 93:12142–12149. [PubMed: 8901547]
9. Tooley CE, Petkowski JJ, Muratore-Schroeder TL, Balsbaugh JL, Shabanowitz J, Sabat M, Minor W, Hunt DF, Macara IG. NRMT is an alpha-N-methyltransferase that methylates RCC1 and retinoblastoma protein. Nature. 2010; 466:1125–1128. [PubMed: 20668449]
10. Webb KJ, Lipson RS, Al-Hadid Q, Whitelegge JP, Clarke SG. Identification of protein N-terminal methyltransferases in yeast and humans. Biochemistry. 2010; 49:5225–5235. [PubMed: 20481588]
11. Alamgir M, Eroukova V, Jessulat M, Xu J, Golshani A. Chemical-genetic profile analysis in yeast suggests that a previously uncharacterized open reading frame, YBR261C, affects protein synthesis. BMC genomics. 2008; 9:583. [PubMed: 19055778]
12. Lee J, Sayegh J, Daniel J, Clarke S, Bedford MT. PRMT8, a new membrane-bound tissue-specific member of the protein arginine methyltransferase family. J Biol Chem. 2005; 280:32890–32896. [PubMed: 16051612]
13. Lucio-Eterovic AK, Singh MM, Gardner JE, Veerappan CS, Rice JC, Carpenter PB. Role for the nuclear receptor-binding SET domain protein 1 (NSD1) methyltransferase in coordinating lysine 36 methylation at histone 3 with RNA polymerase II function. PNAS. 2010; 107:16952–16957. [PubMed: 20837538]

NIH-PA Author Manuscript

NIH-PA Author Manuscript

NIH-PA Author Manuscript

14. Nimura K, Ura K, Shiratori H, Ikawa M, Okabe M, Schwartz RJ, Kaneda Y. A histone H3 lysine 36 trimethyltransferase links Nkx2–5 to Wolf-Hirschhorn syndrome. Nature. 2009; 460:287–291. [PubMed: 19483677]
15. Chen T, Brownawell AM, Macara IG. Nucleocytoplasmic shuttling of JAZ, a new cargo protein for exportin-5. Mol Cell Biol. 2004; 24:6608–6619. [PubMed: 15254228]
16. Shevchenko A, Tomas H, Havlis J, Olsen JV, Mann M. In-gel digestion for mass spectrometric characterization of proteins and proteomes. Nat Protoc. 2006; 1:2856–2860. [PubMed: 17406544]
17. Cox J, Michalski A, Mann M. Software lock mass by two-dimensional minimization of peptide mass errors. J Am Soc Mass Spectrom. 2011; 22:1373–1380. [PubMed: 21953191]
18. Swaney DL, McAlister GC, Coon JJ. Decision tree-driven tandem mass spectrometry for shotgun proteomics. Nat Methods. 2008; 5:959–964. [PubMed: 18931669]
19. Giulietti A, Overbergh L, Valckx D, Decallonne B, Bouillon R, Mathieu C. An overview of real-time quantitative PCR: applications to quantify cytokine gene expression. Methods (San Diego, Calif). 2001; 25:386–401.
20. Kim DE, Chivian D, Baker D. Protein structure prediction and analysis using the Robetta server. Nucleic Acids Res. 2004; 32:W526–531. [PubMed: 15215442]
21. Frederiks F, Tzouros M, Oudgenoeg G, van Welsem T, Fornerod M, Krijgsveld J, van Leeuwen F. Nonprocessive methylation by Dot1 leads to functional redundancy of histone H3K79 methylation states. Nat Struc Mol Biol. 2008; 15:550–557.
22. He C, Li F, Zhang J, Wu J, Shi Y. The methyltransferase NSD3 has chromatin-binding motifs, PHD5-C5HCH, that are distinct from other NSD (nuclear receptor SET domain) family members in their histone H3 recognition. J Biol Chem. 2013; 288:4692–4703. [PubMed: 23269674]
23. Yap DB, Chu J, Berg T, Schapira M, Cheng SW, Moradian A, Morin RD, Mungall AJ, Meissner B, Boyle M, Marquez VE, Marra MA, Gascoyne RD, Humphries RK, Arrowsmith CH, Morin GB, Aparicio SA. Somatic mutations at EZH2 Y641 act dominantly through a mechanism of selectively altered PRC2 catalytic activity, to increase H3K27 trimethylation. Blood. 2011; 117:2451–2459. [PubMed: 21190999]
24. Eisert RJ, Waters ML. Tuning HP1alpha chromodomain selectivity for di- and trimethyllysine. Chembiochem. 2011; 12:2786–2790. [PubMed: 22052799]
25. Stephens PJ, Tarpey PS, Davies H, Van Loo P, Greenman C, Wedge DC, Nik-Zainal S, Martin S, Varela I, Bignell GR, Yates LR, Papaemmanuil E, Beare D, Butler A, Cheverton A, Gamble J, Hinton J, Jia M, Jayakumar A, Jones D, Latimer C, Lau KW, McLaren S, McBride DJ, Menzies A, Mudie L, Raine K, Rad R, Chapman MS, Teague J, Easton D, Langerod A, Lee MT, Shen CY, Tee BT, Huimin BW, Broeks A, Vargas AC, Turashvili G, Martens J, Fatima A, Miron P, Chin SF, Thomas G, Boyault S, Mariani O, Lakhani SR, van de Vijver M, van 't Veer L, Foekens J, Desmedt C, Sotiriou C, Tutt A, Caldas C, Reis-Filho JS, Aparicio SA, Salomon AV, Borresen-Dale AL, Richardson AL, Campbell PJ, Futreal PA, Stratton MR. The landscape of cancer genes and mutational processes in breast cancer. Nature. 2012; 486:400–404. [PubMed: 22722201]
26. Grasso CS, Wu YM, Robinson DR, Cao X, Dhanasekaran SM, Khan AP, Quist MJ, Jing X, Lonigro RJ, Brenner JC, Asangani IA, Ateeq B, Chun SY, Siddiqui J, Sam L, Anstett M, Mehra R, Prensner JR, Palanisamy N, Ryslik GA, Vandin F, Raphael BJ, Kunju LP, Rhodes DR, Pienta KJ, Chinnaiyan AM, Tomlins SA. The mutational landscape of lethal castration-resistant prostate cancer. Nature. 2012; 487:239–243. [PubMed: 22722839]
27. Imielinski M, Berger AH, Hammerman PS, Hernandez B, Pugh TJ, Hodis E, Cho J, Suh J, Capelletti M, Sivachenko A, Sougnez C, Auclair D, Lawrence MS, Stojanov P, Cibulskis K, Choi K, de Waal L, Sharifnia T, Brooks A, Greulich H, Banerji S, Zander T, Seidel D, Leenders F, Ansen S, Ludwig C, Engel-Riedel W, Stoelben E, Wolf J, Goparju C, Thompson K, Winckler W, Kwiatkowski D, Johnson BE, Janne PA, Miller VA, Pao W, Travis WD, Pass HI, Gabriel SB, Lander ES, Thomas RK, Garraway LA, Getz G, Meyerson M. Mapping the hallmarks of lung adenocarcinoma with massively parallel sequencing. Cell. 2012; 150:1107–1120. [PubMed: 22980975]
28. Sabates-Bellver J, Van der Flier LG, de Palo M, Cattaneo E, Maake C, Rehrauer H, Laczko E, Kurowski MA, Bujnicki JM, Menigatti M, Luz J, Ranalli TV, Gomes V, Pastorelli A, Faggiani R, Anti M, Jiricny J, Clevers H, Marra G. Transcriptome profile of human colorectal adenomas. Mol Cancer Res. 2007; 5:1263–1275. [PubMed: 18171984]

NIH-PA Author Manuscript

NIH-PA Author Manuscript

NIH-PA Author Manuscript

29. Kaiser S, Park YK, Franklin JL, Halberg RB, Yu M, Jessen WJ, Freudenberg J, Chen X, Haigis K, Jegga AG, Kong S, Sakthivel B, Xu H, Reichling T, Azhar M, Boivin GP, Roberts RB, Bissahoyo AC, Gonzales F, Bloom GC, Eschrich S, Carter SL, Aronow JE, Kleimeyer J, Kleimeyer M, Ramaswamy V, Settle SH, Boone B, Levy S, Graff JM, Doetschman T, Groden J, Dove WF, Threadgill DW, Yeatman TJ, Coffey RJ Jr, Aronow BJ. Transcriptional recapitulation and subversion of embryonic colon development by mouse colon tumor models and human colon cancer. Genome Biol. 2007; 8:R131. [PubMed: 17615082]

30. Finak G, Bertos N, Pepin F, Sadekova S, Souleimanova M, Zhao H, Chen H, Omeroglu G, Meterissian S, Omeroglu A, Hallett M, Park M. Stromal gene expression predicts clinical outcome in breast cancer. Nat Med. 2008; 14:518–527. [PubMed: 18438415]

31. Jaiswal BS, Janakiraman V, Kljavin NM, Chaudhuri S, Stern HM, Wang W, Kan Z, Dbouk HA, Peters BA, Waring P, Dela Vega T, Kenski DM, Bowman KK, Lorenzo M, Li H, Wu J, Modrusan Z, Stinson J, Eby M, Yue P, Kaminker JS, de Sauvage FJ, Backer JM, Seshagiri S. Somatic mutations in p85alpha promote tumorigenesis through class IA PI3K activation. Cancer Cell. 2009; 16:463–474. [PubMed: 19962665]

32. Nikolsky Y, Sviridov E, Yao J, Dosymbekov D, Ustyansky V, Kaznacheev V, Dezso Z, Mulvey L, Macconaill LE, Winckler W, Serebryiskaya T, Nikolskaya T, Polyak K. Genome-wide functional synergy between amplified and mutated genes in human breast cancer. Cancer Res. 2008; 68:9532–9540. [PubMed: 19010930]

NIH-PA Author Manuscript

NIH-PA Author Manuscript

NIH-PA Author Manuscript

Summary Statement

We have verified the existence of a second mammalian N-terminal methyltransferase (NRMT2) and shown it has a different catalytic activity from and can prime for its previously identified homolog (NRMT1).

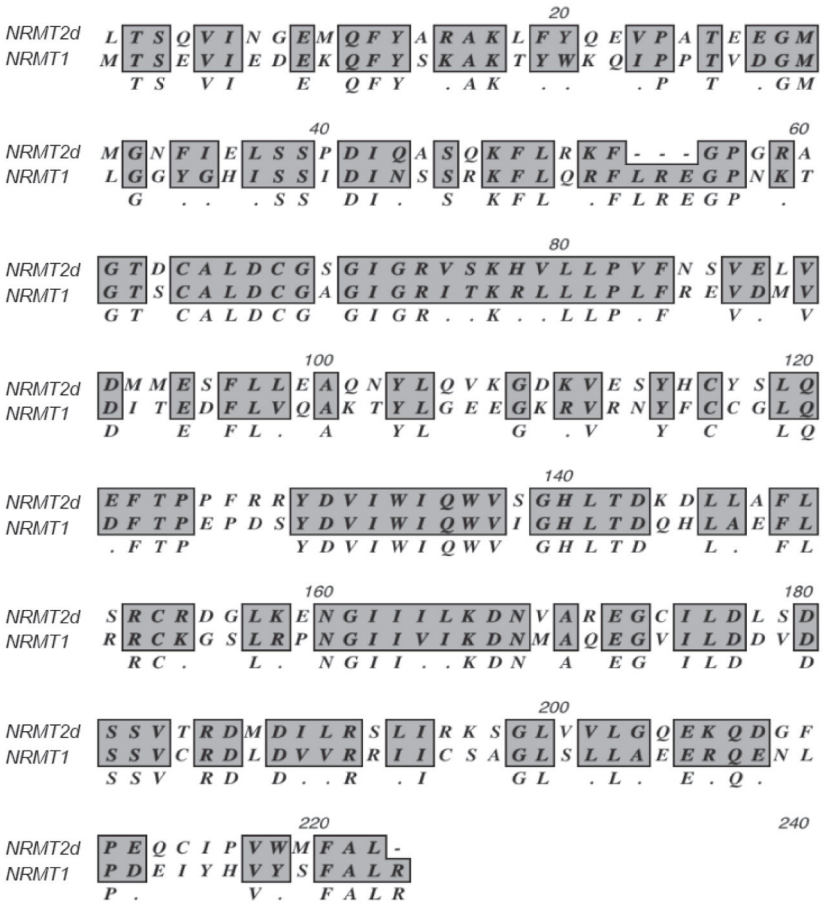

Figure 1. NRMT2 is a close ortholog of NRMT1

Multiple sequence alignment of truncated NRMT2 (NRMT2d - which lacks the 60 amino acid N-terminal domain) and NRMT1 shows sequence identity as high as 50% and sequence similarity at 75%. Identical and similar amino acids are in shaded gray boxes.

NIH-PA Author Manuscript NIH-PA Author Manuscript NIH-PA Author Manuscript

NIH-PA Author Manuscript

NIH-PA Author Manuscript

NIH-PA Author Manuscript

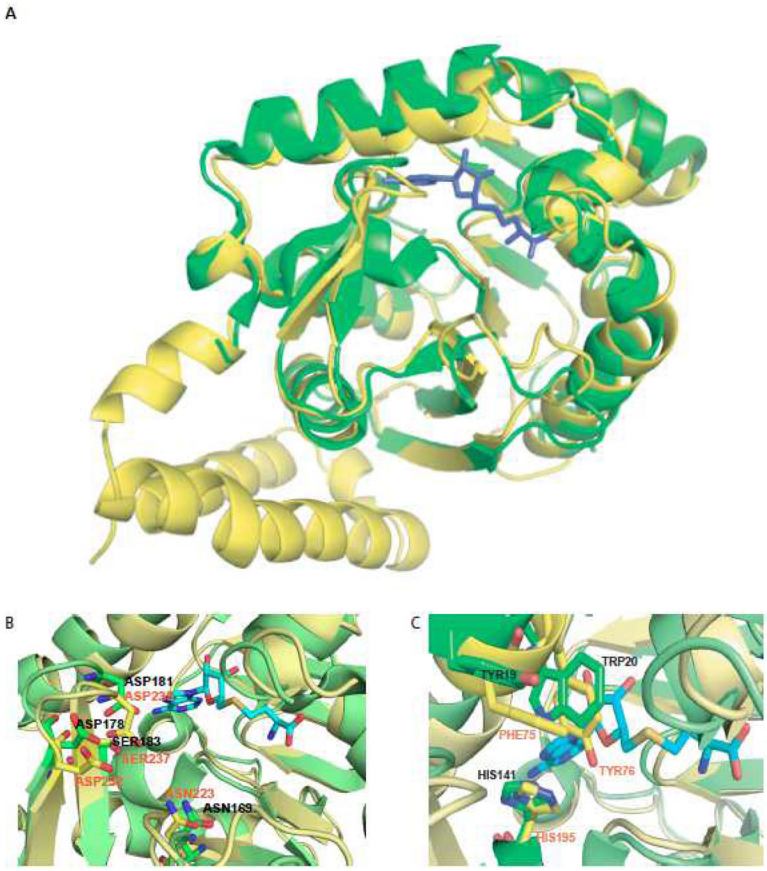

Figure 2. NRMT2 and NRMT1 are structurally similar

(**A**) Homology-based model (as calculated by Robetta server) of NRMT2 molecule (yellow) having the same overall fold as NRMT1 crystal structure (green). Position of the SAH molecule in the NRMT1 crystal structure is shown in blue. The N-terminal 60 amino acid domain of NRMT2, which is not present in NRMT1, is modeled as two helices. (**B**) Critical catalytic residues in NRMT2 (orange font) occupy the same spatial positions as in the NRMT1 crystal structure (black font). (**C**) Conserved aromatic resides in NRMT1 and NRMT2 form a chromodomain-like arrangement of aromatic residues and may be responsible for binding methylated substrates and products.

NIH-PA Author Manuscript
NIH-PA Author Manuscript
NIH-PA Author Manuscript

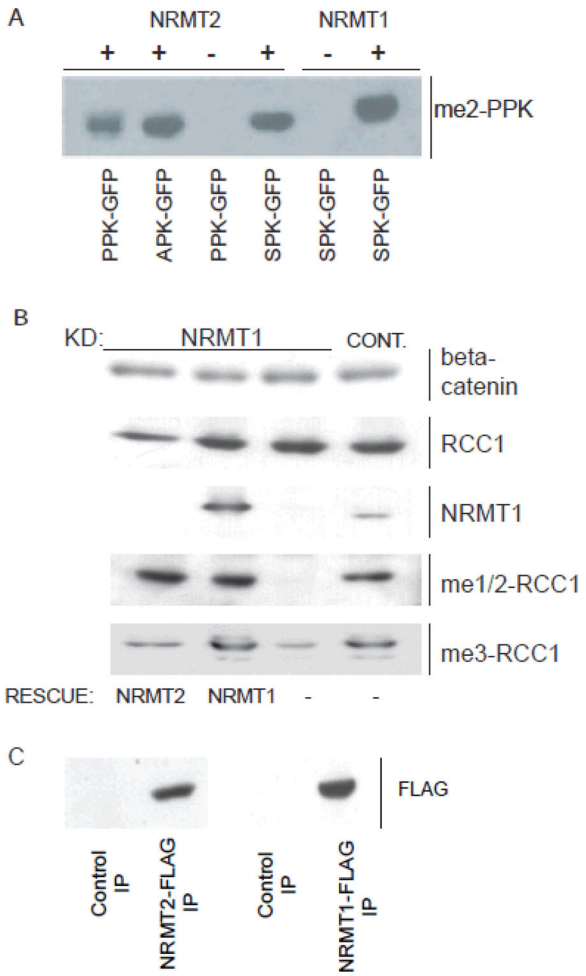

Figure 3. Substrate specificity of NRMT2 is similar to NRMT1

(**A**) *In vitro* methylation reactions showing recombinant murine NRMT2 fused to His-tag and GFP can methylate the same N-terminal consensus sequences (SPK-, APK-, and PPK-RCC1) as recombinant NRMT1. (**B**) Expression of murine NRMT2-FLAG rescues RCC1 mono/dimethylation levels in NRMT1 knockdown cells, but not RCC1 trimethylation. Anti-β-catenin is used as a loading control. (**C**) Anti-FLAG co-immunoprecipitation demonstrating both the NRMT1 and NRMT2 rescue constructs are expressed.

NIH-PA Author Manuscript
NIH-PA Author Manuscript
NIH-PA Author Manuscript

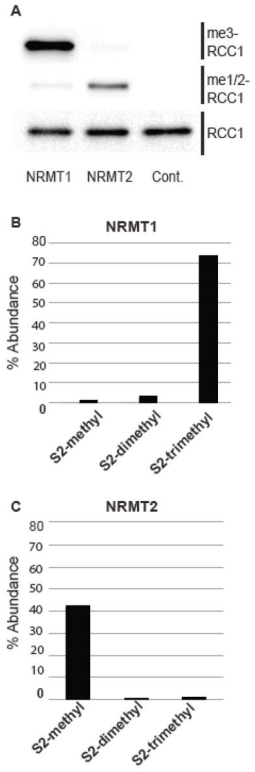

Figure 4. NRMT2 is an N-terminal monomethylase

(**A**) *In vitro* methylation assays of recombinant human RCC1 showing that after 60 min human recombinant NRMT1 produces a significant amount of trimethylated RCC1 with some mono/dimethylated RCC1 remaining. In contrast, under the same conditions, human recombinant NRMT2 only produces mono/dimethylated RCC1 and no trimethylation. (**B** and **C**) Mass spectrometry analysis of identical reactions, confirming that of the recombinant RCC1 with a cleaved initiating methionine, (**B**) NRMT1 trimethylates 75%, dimethylates 3%, and monomethylates 1%. (**C**) NRMTII monomethylates 42% and produces negligible amounts of both di-and trimethylation.

NIH-PA Author Manuscript
NIH-PA Author Manuscript
NIH-PA Author Manuscript

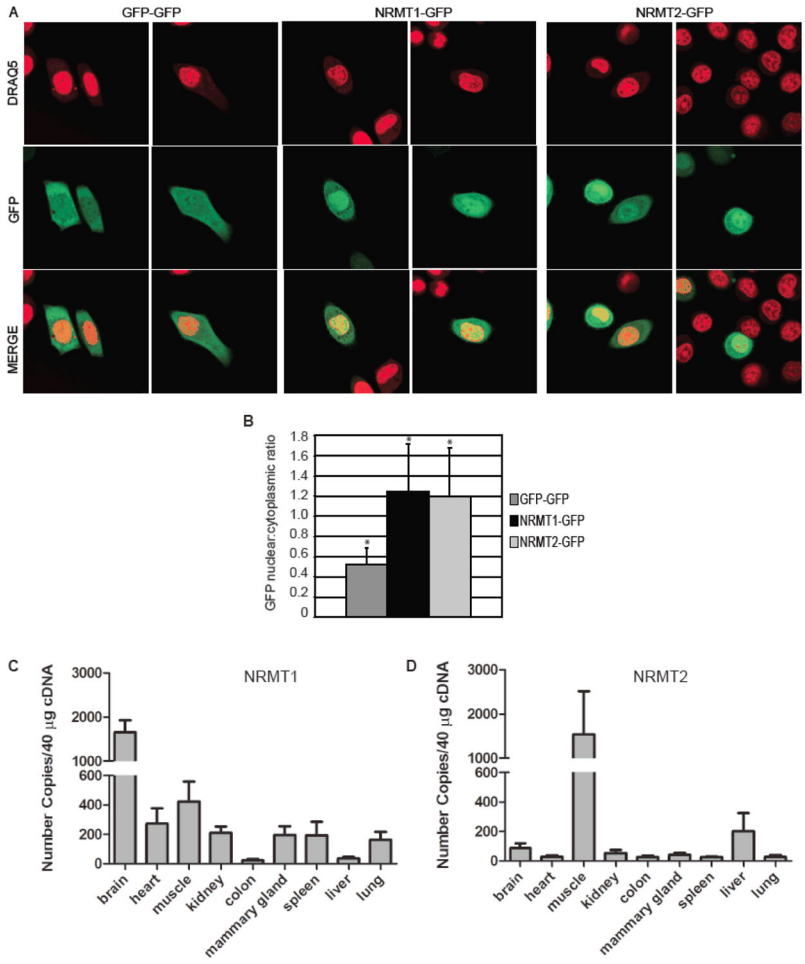

Figure 5. Comparison of NRMT1 and NRMT2 localization and expression patterns

(**A**) NRMT2-GFP and NRMT1-GFP localize in the nuclei of HeLa cells as shown by immunofluorescence, compared to a GFP-GFP control protein. (**B**) Nuclear to cytoplasmic rations were compared to the double GFP fusion protein by two-tailed independent *t* tests. * Indicates P<0.01. n=10 independent samples per construct. Error bars: +/− 1 s.d. (**C**) qRT-PCR analysis of NRMT1 mRNA expression levels in a panel of mouse tissue extracts. Tissues were isolated independently from three female wild type C57BL/6 mice and number of copies determined by standard curve analysis [19]. Error bars denote ± 1 standard error of the mean (s.e.m.). (**D**) qRT-PCR analysis of NRMT2 mRNA expression levels in a panel of mouse tissue extracts. Samples were processed and analyzed as the NRMT1 samples above.

NIH-PA Author Manuscript
NIH-PA Author Manuscript
NIH-PA Author Manuscript

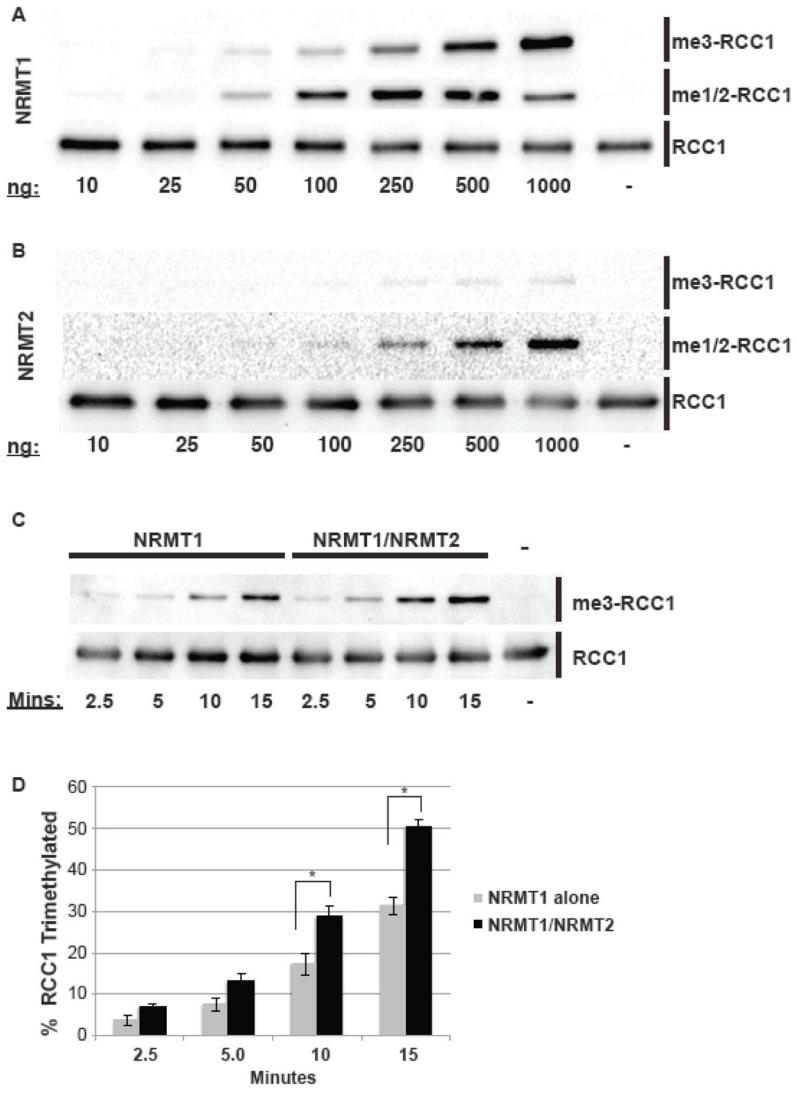

Figure 6. NRMT1 is a distributive methyltransferase whose trimethylation activity is enhanced by the presence of NRMT2

(**A**) *In vitro* methylation reactions with increasing concentrations of recombinant human NRMT1 show first the appearance of mono/dimethylated RCC1, followed by a gradual increase in RCC1 trimethylation and corresponding decrease of mono/dimethylation. (-) Denotes the no enzyme control. (**B**) The same reactions with recombinant human NRMT2 show a slow increase in RCC1 mono/dimethylation and no accumulation of RCC1 trimethylation. (**C**) Combining the two enzymes in the presence of excess substrate results in a faster and more abundant production of trimethylated RCC1 as compared to NRMT1 alone, indicating NRMT2 is priming substrates for NRMT1 trimethylation. (**D**) Quantification of the increase in RCC1 trimethylation in the presence of NRMT2. Error bars represent ± 1 s.e.m. Data were analyzed by two-tailed independent *t* tests, * $p<0.05$. n = 3.